Magnetic order and electronic structure of $5d^3$ double perovskite Sr_2ScOsO_6

A. E. Taylor,[1] R. Morrow,[2] D. J. Singh,[3] S. Calder,[1] M. D. Lumsden,[1] P. M. Woodward,[2] and A. D. Christianson[1,4]

[1] *Quantum Condensed Matter Division, Oak Ridge National Laboratory, Oak Ridge, TN 37831, USA*
[2] *Department of Chemistry, The Ohio State University, Columbus, OH 43210-1185, USA*
[3] *Materials Science and Technology Division, Oak Ridge National Laboratory, Oak Ridge, TN 37831, USA*
[4] *Department of Physics and Astronomy, University of Tennessee, Knoxville, TN 37996, USA*

The magnetic susceptibility, crystal and magnetic structures, and electronic structure of double perovskite Sr_2ScOsO_6 are reported. Using both neutron and x-ray powder diffraction we find that the crystal structure is monoclinic $P2_1/n$ from 3.5 to 300 K. Magnetization measurements indicate an antiferromagnetic transition at $T_N = 92$ K, the highest transition temperature of any double perovskite hosting only one magnetic ion. Type I antiferromagnetic order is determined by neutron powder diffraction, with an Os moment of only $1.6(1)\,\mu_B$, close to half the spin-only value for a crystal field split $5d$ electron state with $t_{2g}{}^3$ ground state. Density functional calculations show that this reduction is largely the result of strong Os-O hybridization, with spin-orbit coupling responsible for only a $\sim 0.1\,\mu_B$ reduction in the moment.

PACS numbers: 75.25.-j, 71.15.Mb, 71.70.Ej

It is important to understand the nature of the d^3 electronic state, as it appears to produce the highest magnetic transition temperatures found in perovskite systems [1]. Perovskites $NaOsO_3$, $5d^3$, and $SrTcO_3$, $4d^3$, have $T_N = 411$ K and $T_N \approx 1000$ K, respectively [2–5]. In the double perovskite Sr_2CrOsO_6 two d^3 ions are present, Cr^{3+} $3d^3$ and Os^{5+} $5d^3$, and a ferrimagnetic transition with $T_C = 725$ K is found, the highest known transition temperature in any double perovskite [6]. However, the presence of two magnetic ions in Sr_2CrOsO_6 makes the interactions controlling this high-T_C insulator more difficult to unravel [7]. It is clear that the influence of the Os $5d^3$ electrons must be understood in order to ultimately understand the high-T_C found in Sr_2CrOsO_6.

The d^3 electronic configuration in a perovskite-type structure is, at first sight, an unlikely host of complex magnetic behavior. The octahedral environment splits the d orbitals into t_{2g} and e_g levels, stabilizing a half occupied $t_{2g}{}^3$ configuration. This is normally assumed to be fully orbitally quenched, resulting in a relatively classical $S = 3/2$ moment behavior [8]. However, many investigations in $4d^3$ and $5d^3$ compounds have found that the ordered magnetic moment measured by neutron diffraction is significantly reduced from the spin only value of $\mu = 3\,\mu_B$ [3, 9–14]. Explanations of this reduced moment have centered on covalency and frustration. It has recently been suggested, however, that the effect of spin-orbit coupling (SOC) cannot be ignored in $4d^3$ and $5d^3$ systems [15]. In Ref. [15] they find that the electronic state may lie between L-S and J-J coupling regimes, and therefore the $t_{2g}{}^3$ assumption is invalid. Recent experimental investigations have therefore discussed the role of SOC in $4d^3$ and $5d^3$ double perovskites [9, 16–18].

Here we investigate the magnetic insulator Sr_2ScOsO_6, which has the highest known magnetic transition temperature in any double perovskite hosting only one magnetic ion [19]. It is the $3d^0 - 5d^3$ analogue of $3d^3 - 5d^3$ Sr_2CrOsO_6, and thus serves as a model system to unravel the behavior of d^3 Os^{5+}. X-ray absorption measurements are consistent with an Os^{5+} valence state and large 3.6 eV t_{2g} to e_g splitting in Sr_2ScOsO_6 [20]. We confirm an antiferromagnetic (AFM) like peak in the susceptibility [13], and by neutron powder diffraction (NPD) we show that this is the result of type I AFM ordering at $T_N = 92$ K. The magnetic moment on the osmium site is $1.6 \pm 0.1\,\mu_B$. This is significantly reduced from the spin-only value, as is the case for $NaOsO_3$ [$\mu_{Os} = 1.0(1)\,\mu_B$] and $SrTcO_3$ [$\mu_{Tc} = 1.87(4)\,\mu_B$], Sr_2CrOsO_6 [$\mu_{Os} = 0.7(3)\,\mu_B$] and other $4d$ and $5d$ double perovskites. Density functional theory (DFT) calculations show that the reduction in moment in Sr_2ScOsO_6 is largely the result of strong Os–O hybridization, with SOC responsible for only a small fraction of the reduction.

Polycrystalline Sr_2ScOsO_6 was synthesized by combining stoichiometric quantities of SrO_2, Os, OsO_2 and Sc_2O_3. Ground mixtures were contained in alumina tubes and sealed in evacuated silica vessels for heatings of 48 hours at 1000 °C. This was followed by regrinding and identical reheating an additional three times.

Magnetization measurements were conducted using a MPMS SQUID magnetometer, from 5 to 400 K under an applied field of 1 kOe. Laboratory x-ray powder diffraction (XRPD) measurements were conducted at room temperature on a Bruker D8 advance using a Ge(111) monochromator and a Cu radiation source ($\lambda = 1.54056$ Å).

NPD measurements were conducted on POWGEN at the Spallation Neutron Source at Oak Ridge National Laboratory (ORNL) [21]. The 0.906 g sample was contained in a vanadium can and measured at 10 K and 300 K. The chopper settings were chosen to correspond to a measured d-spacing range of 0.2760–3.0906 Å. NPD and XRPD data were analyzed using the Rietveld method as implemented in GSAS+EXPGUI [22, 23].

To determine the magnetic structure, separate NPD measurements were performed using a 6 g sample on HB-2A at the High Flux Isotope Reactor at ORNL [24]. The sample was sealed in a vanadium can with He exchange gas, and a closed cycle refrigerator was used to

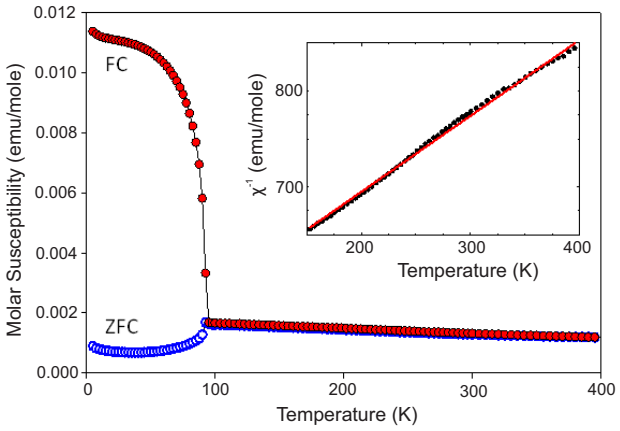

Figure 1. (Color online) Temperature dependence of the susceptibility measured in a 1 kOe applied field. Blue open symbols and red closed symbols show the zero field cooled (ZFC) and field cooled (FC) [at 1 kOe] measurements, respectively. The inset shows the inverse susceptibility well above T_N, and the result of a Curie-Weiss fit to the data (solid line).

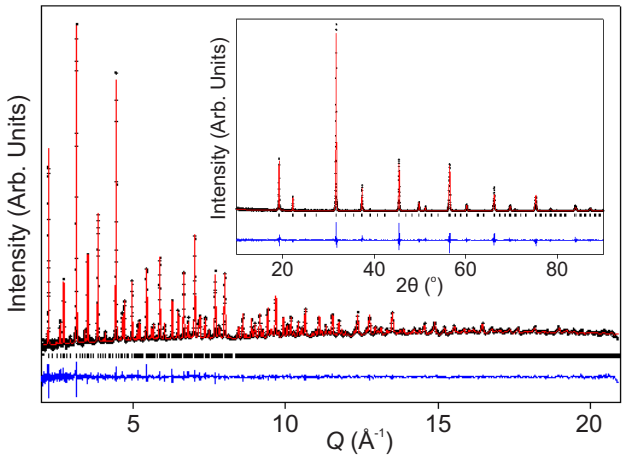

Figure 2. (Color online) Rietveld refinements against data (black crosses), collected at room temperature by NPD on POWGEN (main panel) and XRPD (inset). The difference between calculation and data is also shown, and is offset for clarity.

reach 3.5 K. Measurements were conducted with a neutron wavelength of 2.4137 Å, with collimation of 12′–open–12′. The resulting data were analyzed with the Rietveld refinement suite Fullprof [25], using the magnetic form factor for Os^{5+} from Ref. [26].

A peak at 92.5 K is seen in the ZFC susceptibility data, see Fig. 1, which is characteristic of AFM order. The FC data shows a ferromagnetic component, that is likely the result of a small canting of the magnetic moments. At 5 K the ZFC M versus H measured up to 5 T (not shown) shows a linear relation consistent with AFM order. These results are similar to the magnetization measurements recently reported in Ref. [13]. Earlier magnetization measurements show a peak in the susceptibility at 25 K, which may be due to different sample quality, as a cubic symmetry was determined from XRPD [20]. The inverse susceptibility versus temperature in the paramagnetic region for our sample is shown in the inset to Fig. 1, along with a Curie-Weiss fit to the data. The fit yields a Curie-Weiss temperature $\Theta = -677$ K and an effective moment of $\mu_{eff} = 3.18\,\mu_B$. The reduction in the effective moment from the expected spin-only value of $\mu_{eff} = 3.87\,\mu_B$ (assuming a g-factor of 2) is likely an indication of SOC acting as a perturbation on the $t_{2g}{}^3$ state. The frustration index for Sr_2ScOsO_6 is $|\Theta|/T_N = 7.4$, indicating a high degree of frustration as expected for a near face-centered-cubic arrangement of magnetic ions.

The results of XRPD measurements and Rietveld analysis are presented in the inset to Fig. 2. As Sc and Os have significantly different atomic masses, x-rays are particularly sensitive to anti-site mixing between B and B' sites. We find that the sites are fully occupied, with 0.952(4) Os [Sc] and 0.048(4) Sc [Os] occupancy on the B' [B] site. Some anti-site disorder is unsurprising given that the ratio of ionic radii of Sc^{3+}/Os^{5+} is smaller than 100 % ordered Os double perovskites [13, 27]. The occupancies determined from XRPD were subsequently used in the NPD structural refinements. NPD is advantageous for a full structural refinement due to a greater sensitivity to the oxygen positions in the system.

The data from NPD on POWGEN at 300 K are shown in the main panel of Fig. 2. While the metric of the unit cell was highly pseudocubic, the space group symmetry was determined by the presence of X point reflections in the NPD pattern (two odd indices and one even as indexed on a 2×2×2 perovskite cell) [28] as the common monoclinic $P2_1/n$ [29] with the tilt system $a^-a^-c^+$ [30]. The Wykcoff positions of the atoms are: Sc on 2d (½ 0 0), Os on 2c (0 ½ 0), and Sr, O1, O2 and O3 on 4e sites (x y z). Due to the high degree of pseudosymmetry, there was reduced sensitivity to the refinement of the oxygen positional parameters. Soft constraints were therefore placed on the bond lengths with the weakest weighting, using values of 2.06 and 1.96 Å in accordance with Sc–O and Os–O bond lengths found in similar double perovskites [6, 28]. The introduction of soft constraints results in only a marginal difference in the quality of the refinement (R_{wp} is increased by only 0.02 to 4.32 %). However, if the soft constraints are removed unphysical bond lengths result. We find that space group $P2_1/n$ describes the structure down to 3.5 K, with no evidence for any structural phase transition. Previous reports of the crystal structure were only available from XRPD at room temperature [13, 20]. Our results agree with the space group $P2_1/n$ reported in Ref. [13], but we find the monoclinic angle $\beta = 90.218(3)°$ to be significantly larger than their result, $\beta = 90.083(2)°$. The complete structural results from the Rietveld refinements for 300 K and 10 K are given in Table I and [31].

Having determined the crystal structure of Sr_2ScOsO_6, we now turn to discussion of the magnetic structure. Fig-

Temperature (K)	10 K	300 K
Space Group	$P2_1/n$	$P2_1/n$
a (Å)	5.6398(2)	5.6465(2)
b (Å)	5.6373(2)	5.6477(2)
c (Å)	7.9884(3)	8.0037(3)
V (Å^3)	253.98(2)	255.24(2)
β	90.219(2)°	90.218(3)°
R_{wp}	5.41 %	4.32 %
Sr x	0.004(1)	0.004(2)
Sr y	-0.0142(5)	-0.006(2)
Sr z	0.2506(8)	0.250(1)
O1 x	0.2202(7)	0.232(1)
O1 y	0.2295(7)	0.220(1)
O1 z	0.0270(7)	0.0257(8)
O2 x	0.245(1)	0.2409(9)
O2 y	0.233(1)	0.2523(9)
O2 z	0.4757(9)	0.4836(9)
O3 x	0.5443(8)	0.5423(9)
O3 y	0.006(1)	-0.007(2)
O3 z	0.2558(4)	0.2454(3)

Table I. Results from Rietveld refinements of NPD data from POWGEN, as described in the text.

ure 3(a) shows data collected on HB-2A at temperatures both above T_N (115 K) and below T_N (85 K and 3.5 K). Peaks at $Q = 0.78$ and 1.1 Å can be seen to develop in the $T < T_N$ data sets, which are not present at 115 K. These reflections can be indexed as (0 0 1) and (1 0 0) or (0 1 0) respectively, indicating a magnetic propagation vector $\mathbf{k} = (0\,0\,0)$. There are two irreducible representations in this case, Γ_1 and Γ_3, compatible with the $P2_1/n$ symmetry with Os on the 2c Wyckoff site, each representing a simple type I AFM structure. Type I order is favored in double perovskites when the nearest neighbor (NN) Os-O-O-Os exchange is dominant, type II order results if the next nearest neighbor (NNN) Os-Sc-Os interaction is stronger, as found in some 3d ion compounds [19, 32].

The type I magnetic model with moments in the a-b plane was fit to the data, with the result shown in Fig. 3(b). As the monoclinic distortion is small, it is not possible to determine the direction of the magnetic moment in the a-b plane from the powder data. The magnetic structure is shown in Fig. 3(d) with the spins represented along the a-axis. The size of the Os moment extracted from the fit is $\mu_{Os} = 1.6(1)\,\mu_B$, assuming a 95 % Os occupancy of the B' site is contributing to the scattering. Significant covalency may explain the observation of a greatly reduced moment determined by neutron scattering as compared to μ_{eff} from magnetization measurements [33]. The detailed temperature evolution of the $Q_{(001)} = 0.78$ Å peak is shown in Fig. 3(c), along with a power-law curve that was fit to the data. This confirms the T_N= 92(1) K transition temperature associated with this magnetic peak.

It is informative to put these results in context against other double perovskites which host a d^0d^3 configuration. Despite high frustration indexes $|\Theta|/T_N$, most of these systems overcome frustration to order in a type I AFM state at low temperature [see Fig. 3(d)], although some show short range incommensurate order or type III order [9, 11, 13, 17, 34, 35]. Sr_2ScOsO_6, Sr_2YOsO_6 and Ba_2YOsO_6 all host long range type I AFM order, with T_Ns of 95 K, 53 K and 69 K, and frustration indexes $|\Theta|/T_N$ = 7.4, 6.4 and 11 respectively [13, 17]. Ba_2YOsO_6 is the only one of these compounds to maintain a cubic symmetry, which likely explains the higher level of frustration found in this system [17]. Sr_2ScOsO_6 and Ba_2YOsO_6 have the same size magnetic moment as determined by neutron diffraction, 1.6(1) μ_B and 1.65(6) μ_B, and so it seems likely that the Os d electrons are in the same state in each of these materials, explaining the relatively high T_Ns observed in both. It would seem that the monoclinic distortion in Sr_2ScOsO_6 relieves frustration and, along with a smaller unit cell parameter, allows this material to host the highest ordering temperature. The presence of a small amount of Sc/Os site disorder in Sr_2ScOsO_6 may also act to enhance T_N, as the interactions between anti-site Os ions and regular site Os neighbors will be strongly AFM.

It is unclear, however, why Sr_2YOsO_6 has the lowest T_N of the three compounds. Its lattice is intermediate in size between Sr_2ScOsO_6 and Ba_2YOsO_6, which in principle implies strengthened NN interactions over Ba_2YOsO_6. Also, its magnetic moment is larger at 1.91(3) μ_B [13] which should energetically favor a higher T_N. In the monoclinic symmetry the 12 NN Os distances are not equal, and in Sr_2YOsO_6 the shortest distance is between in-plane ferromagnetically aligned pairs, whereas in Sr_2ScOsO_6 the shortest distance is for out-of-plane AFM aligned pairs. This might explain some lowering of T_N in Sr_2YOsO_6, but does not explain the larger magnetic moment. This raises the possibility that a single mechanism both causes a reduction in μ and enhances the exchange interactions and therefore increases T_N, as reflected in Sr_2ScOsO_6 and Ba_2YOsO_6. The similar Ru-based compounds Ba_2YRuO_6 and Sr_2YRuO_6 have larger moments of $\sim 2\,\mu_B$ and lower T_Ns of ~ 30 K [11, 35, 36], whereas high-T_N $NaOsO_3$ also has a reduced moment [3]. Increased hybridization between Os 5d orbitals and O 2p orbitals could be responsible, as this reduces the localized Os moment, but could increase the exchange coupling along the nearest neighbor Os-O-O-Os pathway.

To investigate the effect of hybridization in Sr_2ScOsO_6, we have performed DFT calculations using the experimental crystal structure. The calculations were done using the general potential linearized augmented planewave (LAPW) method, [37] as implemented in the WIEN2k code [38]. We used the generalized gradient approximation (GGA) of Perdew, Burke and Ernzerhof [39], both by itself and including a Coulomb repulsion via the GGA+U scheme, with U=3 eV. SOC was included in the calculations. We find an AFM ground state in agreement with the experimental observation, and confirm that covalency is largely responsible for the reduction of the Os moment well below the $t_{2g}{}^3$ spin-only value.

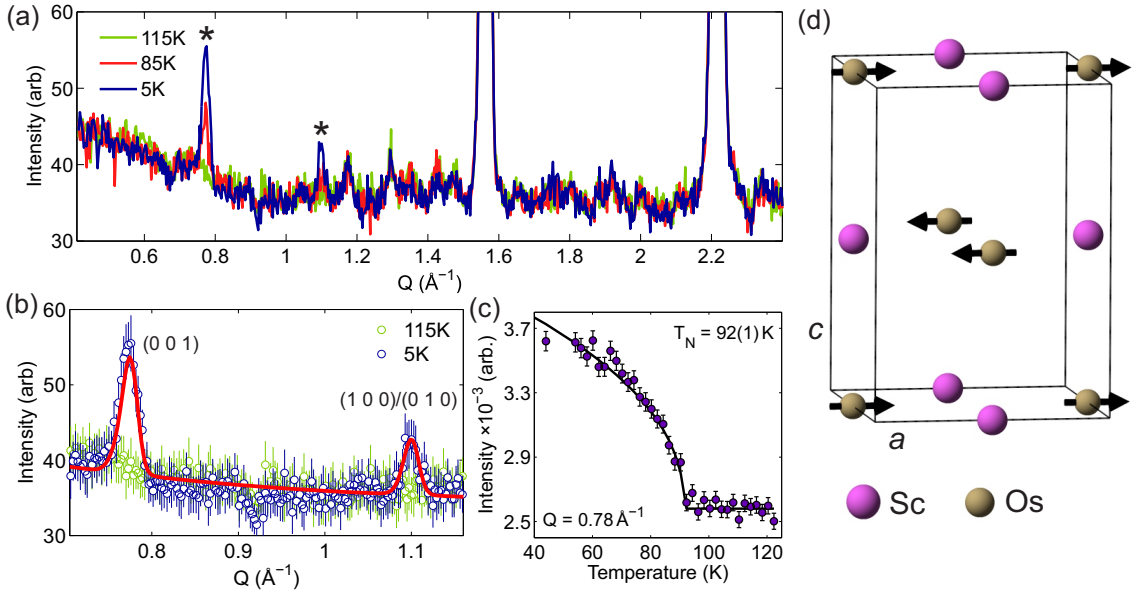

Figure 3. (Color online) (a) NPD data collected with HB-2A at 115 K ($>T_N$), and 85 and 3.5 K ($<T_N$). Magnetic peaks are indicated by stars. (b) Results of Rietveld refinements of the 3.5 K data (solid line). (c) Intensity of scattering at $Q = 0.78$ Å against temperature (circles). The line is the result of a power-law fit against the data. The intensity is number of counts measured with the $Q = 0.78$ Å peak counted for 10 minutes per point. (d) The magnetic structure in one unit cell of Sr_2ScOsO_6, showing only Os and Sc ions. Moments are depicted along a, but their direction within the a-b plane is unknown.

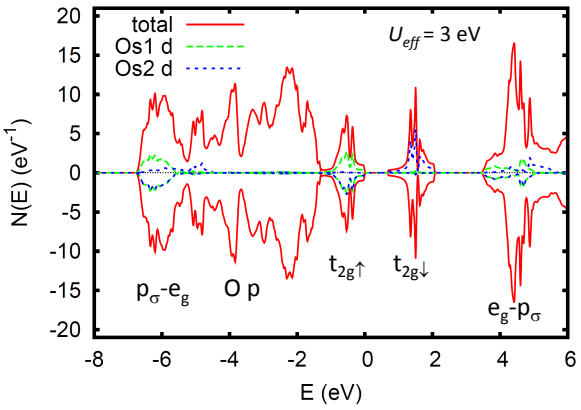

Figure 4. (Color online) Calculated density of states and Os d projections, from GGA+U calculations including spin-orbit. Os1 and Os2 denote the up and down spin Os relative to the global direction (set along the a-axis). The projections are per atom for a given spin, while the total is per spin for the two Os atom unit cell.

The density of states from the GGA+U calculation is shown in Fig. 4. Even with the inclusion of U there is an exceptionally strong hybridization between Os $5d$ and O $2p$ states evident in the projections. This hybridization provides a mechanism for relatively high ordering temperatures despite the large separation between Os magnetic ions in the double perovskite structure. Specifically, it leads to a redistribution of the moment to include sizable moments on the O ions, with the $\sim 3\ \mu_B$ of spin moment spread over OsO_6 that form effective magnetic clusters. These magnetic clusters are in close proximity and are therefore strongly interacting. This is similar to the clusters found in the related double perovskite Sr_2YRuO_6 with $T_N = 26$ K [40], but the hybridization is stronger in the present case.

From the GGA+U calculation we find an Os moment of $1.8\,\mu_B$, without U it is only $1.4\,\mu_B$. The calculated orbital moment is reasonably large, $-0.11\,\mu_B$ in both cases, but the major reduction in the Os moment appears to result from hybridization. This agrees with the experimental finding that the moment observed via neutron scattering is greatly reduced from the $t_{2g}{}^3$ spin-only value, but there is only a slight reduction in $\mu_{\rm eff}$ determined from magnetization measurements.

In this report, by combining a full experimental characterization of Sr_2ScOsO_6 with DFT calculations in which we include spin-orbit coupling, we have been able to establish the key properties controlling Sr_2ScOsO_6. The Os $t_{2g}{}^3$ ground state strongly hybridizes with the surrounding oxygen ions, resulting in the highest magnetic transition temperature for a double perovskite hosting a single magnetic ion. A consequence of the hybridization is the dramatically reduced ordered moment observed by neutron diffraction. Spin-orbit coupling appears to play only a minor role. This is indicated by the small reduction in the effective moment from a Curie-Weiss analysis of the susceptibility, as well the minimal effects due to spin-orbit coupling shown by DFT.

ACKNOWLEDGEMENTS

Support for this research was provided by the Center for Emergent Materials an NSF Materials Research Science and Engineering Center (DMR-0820414). The research at ORNL's Spallation Neutron Source and High Flux Isotope Reactor was supported by the Scientific User Facilities Division, Office of Basic Energy Sciences, U.S. Department of Energy (DOE). The theoretical calculations (DJS) were supported by the Department of Energy, Basic Energy Sciences, Materials Sciences and Engineering Division. The authors gratefully acknowledge A. Huq for providing help with the experimental work on Powgen, and J.Q. Yan, D. Mandrus and B. Sales for useful discussions.

[1] S. Middey, A. K. Nandy, S. K. Pandey, P. Mahadevan, and D. D. Sarma, Phys. Rev. B **86**, 104406 (2012).

[2] Y. G. Shi, Y. F. Guo, S. Yu, M. Arai, A. A. Belik, A. Sato, K. Yamaura, E. Takayama-Muromachi, H. F. Tian, H. X. Yang, J. Q. Li, T. Varga, J. F. Mitchell, and S. Okamoto, Phys. Rev. B **80**, 161104 (2009).

[3] S. Calder, V. O. Garlea, D. F. McMorrow, M. D. Lumsden, M. B. Stone, J. C. Lang, J.-W. Kim, J. A. Schlueter, Y. G. Shi, K. Yamaura, Y. S. Sun, Y. Tsujimoto, and A. D. Christianson, Phys. Rev. Lett. **108**, 257209 (2012).

[4] E. E. Rodriguez, F. Poineau, A. Llobet, B. J. Kennedy, M. Avdeev, G. J. Thorogood, M. L. Carter, R. Seshadri, D. J. Singh, and A. K. Cheetham, Phys. Rev. Lett. **106**, 067201 (2011).

[5] G. J. Thorogood, M. Avdeev, M. L. Carter, B. J. Kennedy, J. Ting, and K. S. Wallwork, Dalton Trans. **40**, 7228 (2011).

[6] Y. Krockenberger, K. Mogare, M. Reehuis, M. Tovar, M. Jansen, G. Vaitheeswaran, V. Kanchana, F. Bultmark, A. Delin, F. Wilhelm, A. Rogalev, A. Winkler, and L. Alff, Phys. Rev. B **75**, 020404 (2007).

[7] O. N. Meetei, O. Erten, M. Randeria, N. Trivedi, and P. Woodward, Phys. Rev. Lett. **110**, 087203 (2013).

[8] G. Chen and L. Balents, Phys. Rev. B **84**, 094420 (2011).

[9] A. A. Aczel, D. E. Bugaris, L. Li, J.-Q. Yan, C. de la Cruz, H. zur Loye, and S. E. Nagler, Phys. Rev. B **87**, 014435 (2013).

[10] A. A. Aczel, D. E. Bugaris, J. Yeon, C. de la Cruz, H. zur Loye, and S. E. Nagler, Phys. Rev. B **88**, 014413 (2013).

[11] P. Battle and C. Jones, Journal of Solid State Chemistry **78**, 108 (1989).

[12] S. Calder, M. D. Lumsden, V. O. Garlea, J. W. Kim, Y. G. Shi, H. L. Feng, K. Yamaura, and A. D. Christianson, Phys. Rev. B **86**, 054403 (2012).

[13] A. K. Paul, A. Sarapulova, P. Adler, M. Reehuis, S. Kanungo, D. Mikhailova, W. Schnelle, Z. Hu, C. Kuo, V. Siruguri, S. Rayaprol, Y. Soo, B. Yan, C. Felser, L. Hao Tjeng, and M. Jansen, Z. anorg. allg. Chem. **641**, 197 (2015).

[14] P. Kayser, M. J. Martínez-Lope, J. A. Alonso, M. Retuerto, M. Croft, A. Ignatov, and M. T. Fernández-Díaz, Eur. J. Inorg. Chem. **2014**, 178 (2014).

[15] H. Matsuura and K. Miyake, J. Phys. Soc. Jpn. **82**, 073703 (2013).

[16] J. P. Carlo, J. P. Clancy, K. Fritsch, C. A. Marjerrison, G. E. Granroth, J. E. Greedan, H. A. Dabkowska, and B. D. Gaulin, Phys. Rev. B **88**, 024418 (2013).

[17] E. Kermarrec, C. A. Marjerrison, C. M. Thompson, D. D. Maharaj, K. Levin, S. Kroeker, G. E. Granroth, R. Flacau, Z. Yamani, J. E. Greedan, and B. D. Gaulin, Phys. Rev. B **91**, 075133 (2015).

[18] G. J. Nilsen, C. M. Thompson, G. Ehlers, C. A. Marjerrison, and J. E. Greedan, Phys. Rev. B **91**, 054415 (2015).

[19] S. Vasala and M. Karppinen, Prog. Solid State Chem., in press 10.1016/j.progsolidstchem.2014.08.001.

[20] J.-H. Choy, D.-K. Kim, and J.-Y. Kim, Solid State Ionics **108**, 159 (1998).

[21] A. Huq, J. P. Hodges, O. Gourdon, and L. Heroux, Z. Kristallogr. **1**, 127 (2011).

[22] A. C. Larson and R. B. Von Dreele, "General Structure Analysis System (GSAS)," (1994).

[23] B. H. Toby, J. Appl. Crystallogr. **34**, 210 (2001).

[24] V. O. Garlea, B. C. Chakoumakos, S. A. Moore, G. B. Taylor, T. Chae, R. G. Maples, R. A. Riedel, G. W. Lynn, and D. L. Selby, Appl. Phys. A **99**, 531 (2010).

[25] J. Rodríguez-Carvajal, Physica B **192**, 55 (1993).

[26] K. Kobayashi, T. Nagao, and M. Ito, Acta Crystallogr. A **67**, 473 (2011).

[27] R. Morrow, R. Mishra, O. D. Restrepo, M. R. Ball, W. Windl, S. Wurmehl, U. Stockert, B. Büchner, and P. M. Woodward, J. Am. Chem. Soc. **135**, 18824 (2013).

[28] P. W. Barnes, M. W. Lufaso, and P. M. Woodward, Acta Crystallogr. B **62**, 384 (2006).

[29] M. W. Lufaso, P. W. Barnes, and P. M. Woodward, Acta Crystallogr. B **62**, 397 (2006).

[30] A. M. Glazer, Acta Crystallogr. B **28**, 3384 (1972).

[31] See supplementary information.

[32] P. Battle, G. Blake, T. Gibb, and J. Vente, J. Solid State Chem. **145**, 541 (1999).

[33] J. Hubbard and W. Marshall, Proc. Phys. Soc. **86**, 561 (1965).

[34] C. M. Thompson, J. P. Carlo, R. Flacau, T. Aharen, I. A. Leahy, J. R. Pollichemi, T. J. S. Munsie, T. Medina, G. M. Luke, J. Munevar, S. Cheung, T. Goko, Y. J. Uemura, and J. E. Greedan, J. Phys.: Condens. Matter **26**, 306003 (2014).

[35] P. Battle and W. Macklin, J. Solid State Chem. **52**, 138 (1984).

[36] T. Aharen, J. E. Greedan, F. Ning, T. Imai, V. Michaelis, S. Kroeker, H. Zhou, C. R. Wiebe, and L. M. D. Cranswick, Phys. Rev. B **80**, 134423 (2009).

[37] D. J. Singh and L. Nordstrom, *Planewaves Pseudopotentials and the LAPW Method, 2nd Ed.* (Springer,Berlin, 2006).

[38] P. Blaha, K. Schwarz, G. Madsen, D. Kvasnicka, and J. Luitz, WIEN2k(Tech. Univ. Wien, Austria) (2001).

[39] J. P. Perdew, K. Burke, and M. Ernzerhof, Phys. Rev. Lett. **77**, 3865 (1996).

[40] I. I. Mazin and D. J. Singh, Phys. Rev. B **56**, 2556 (1997).